Title
A Pathogen-Specific Cargo Delivery Platform Based on Mesoporous Silica Nanoparticles

Journal
Journal of the American Chemical Society, 139(19)

ISSN
0002-7863

Authors
Ruehle, Bastian
Clemens, Daniel L
Lee, Bai-Yu
et al.

Publication Date
2017-05-17

DOI
10.1021/jacs.7b01278

A pathogen-specific cargo delivery platform based on mesoporous silica nanoparticles

Journal:	*Journal of the American Chemical Society*
Manuscript ID	ja-2017-012783.R1
Manuscript Type:	Article
Date Submitted by the Author:	11-Apr-2017
Complete List of Authors:	Ruehle, Bastian; University of California Los Angeles, Chemistry & Biochemistry Clemens, Daniel; University of California, Los Angeles, Department of Medicine Lee, Bai-Yu; University of California, Los Angeles, Medicine Horwitz, Marcus; UCLA, Medicine Zink, Jeffrey; UCLA, Chemistry and Biochemistry

A pathogen-specific cargo delivery platform based on mesoporous silica nanoparticles

Bastian Ruehle,[†,$,‡] Daniel L. Clemens,[§,‡] Bai-Yu Lee,[§,‡] Marcus A. Horwitz,[§,*] Jeffrey I. Zink[†,$,*]

† Department of Chemistry & Biochemistry, University of California, Los Angeles, California 90095, United States

$ California NanoSystems Institute, University of California, Los Angeles, California 90095, United States

§ Division of Infectious Diseases, Department of Medicine, University of California, Los Angeles, California 90095, United States

‡ These authors contributed equally

KEYWORDS: Mesoporous Silica Nanoparticles, Infectious Diseases, Drug Delivery, Francisella Tularensis, Antibodies, Lipopolysaccharide

ABSTRACT: We present a synthetic approach to a highly pathogen-selective detection and delivery platform based on the interaction of an antibody nanovalve with a tetrasaccharide from the O-Antigen of the lipopolysaccharide of *Francisella tularensis* bacteria, a Tier 1 Select Agent of bioterrorism. Different design considerations are explored, and proof-of-concept for highly pathogen-specific cargo release from mesoporous silica nanoparticles is demonstrated by comparisons of the release of a signal transducer and model drug by LPS from *Francisella tularensis* vs. *Pseudomonas aeruginosa*, and by *Francisella tularensis* live bacteria vs. the closely related bacterium *Francisella novocida*. In addition to the specific response to a bio-warfare agent, treatment of infectious diseases in general could benefit tremendously from a delivery platform that releases its antibiotic payload only at the site of infection and only in the presence of the target pathogen, thereby minimizing off-target toxicities.

1. Introduction

In this work, we demonstrate a cargo delivery platform that features highly specific cargo release *in vitro* in the presence of the O-Antigen of the lipopolysaccharide (LPS) of *Francisella tularensis* (Ft). Ft, the causative agent of tularemia, is a Tier 1 Select Agent of bioterrorism due to its high infectivity, capacity to cause serious morbidity and mortality,[1–3] and the relative ease with which it can be cultured on a large scale, weaponized, and dispersed into the environment. Ft was developed as a biological warfare agent during World War II by Japan and during the Cold War by both the U.S. and the former Soviet Union.[4–6] Because it can be fatal even with appropriate therapy, there is a need for both detection and responsive therapeutic treatment modalities such as our triggered, pathogen-responsive cargo delivery platform. Additionally, since numerous infectious diseases are caused by Gram-negative bacteria, which harbor LPS in their cell walls, the same design considerations and synthesis procedures could in principle be applied to recognize and respond to many other pathogens.

A cargo delivery platform that releases its payload specifically in the presence of a targeted pathogen would be highly beneficial for selectively detecting and treating infectious diseases. Not only can triggered drug release from a carrier system improve upon treatment with a free drug,[7,8] but a drug delivery platform that additionally releases its cargo only in the presence of a target pathogen could – in addition to signaling the presence of the pathogen in question – enhance efficacy by increasing drug delivery to infected cells while reducing the antibiotic burden on uninfected cells, thereby minimalizing unwanted side effects. Moreover, considering the ever-growing number of infections caused by antibiotic resistant strains of bacteria, many arising from the use of broad spectrum antibiotics, and the adverse health consequences arising from alterations of the human microbiome by such broad-spectrum antibiotics, there is a need for greater selectivity in targeting pathogenic bacteria.

Making a drug delivery platform pathogen-specific poses several challenges. First, it is necessary to consider the "container" used to hold the payload that later is to be released specifically in the presence of the target pathogen. Here, we chose mesoporous silica nanoparticles (MSNs) as the carriers due to their large internal pore volume and surface area, tunable particle size, pore size, and morphology, and huge flexibility for chemical modifications.[9–13] Next, one needs to address how a gatekeeping mechanism can be designed and implemented on this carrier that can act as a cap on the cargo-loaded pores and releases the cargo selectively in response to a specific pathogen. In nature, one way that highly selective recognition of target pathogens is

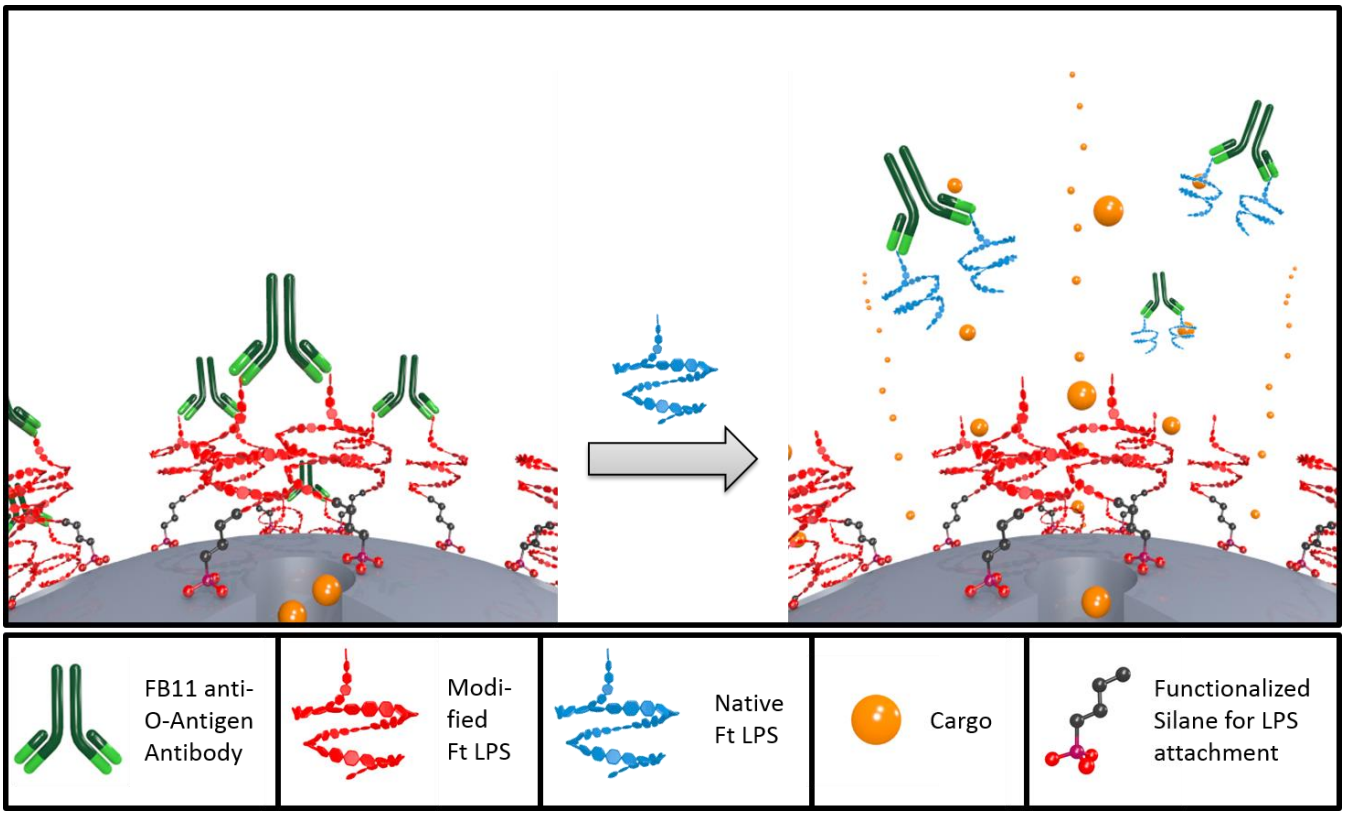

Figure 1. Schematic representation of the triggered release of cargo (orange spheres) loaded into pores due to a competitive displacement of the antibody (green) that caps the pore by naturally occurring *Francisella tularensis* LPS (blue).

achieved is through antibody-antigen interactions, and indeed, MSN-antibody conjugates have been reported that were used for analyte detection,[14–17] theranostics/imaging,[17–22] or cell targeting.[23–28] However, these examples demonstrate a specific recognition of an antigen by the MSN-antibody conjugate, but the recognition event itself does not stimulate a signal or killing response, i.e., there is no antigen-responsive gatekeeping mechanism that would selectively control cargo release only in the presence of a specific antigen or pathogen.

A design that can be used to achieve a proactive response is one in which the antibody is bound to antigens immobilized on the surface of the MSNs, consequently acting as a "cap" that hinders the diffusion of cargo from the pores of the container. By subtle manipulation of the surface-bound antigen such that the affinity of the antibody binding to it is reduced, the antigen produced by the target pathogen can compete effectively for binding to the gatekeeper antibody, leading to displacement of the antibody, pore uncapping and cargo release (Figure 1). The feasibility of this approach has been demonstrated for the detection of compounds such as sulfonamides,[29] finasteride,[30] and triacetone triperoxide,[31] but to the best of our knowledge, a triggered release of cargo from MSNs by antigens that are naturally produced by bacteria has not been demonstrated. For the triggering event to occur, a way to "tune" the rather strong noncovalent antibody-antigen interaction is required such that a competitive displacement of the antibody cap occurs even at low antigen concentrations and at the same time there is minimal non-specific cargo release due to "leakage" from the delivery platform.

For our platform, we used the interaction of the FB11 antibody with a derivative of the O-antigen of Ft LPS immobilized on the nanoparticle surface for selective, pathogen-induced cargo release in our gated nanoparticle design. In the presence of the O-Antigen that is naturally produced and shed by Ft (Figure S1), a competitive displacement of the antibody cap takes place, which leads to pore uncapping and cargo release (Figure 1).

2. Experimental section

Unfunctionalized mesoporous silica nanoparticles were synthesized according to a published procedure.[32] Functionalization was done by refluxing the unfunctionalized nanoparticles with the respective trialkoxysilane in dry toluene under an inert atmosphere of dry nitrogen overnight. The CTAB template was extracted from the pores using two extraction steps with ethanolic ammonium nitrate and in some cases ethanolic HCl solutions. The O-Antigen was coupled to amine-functionalized MSNs through EDC/NHS amidation or to ICPTES functionalized MSNs in dry DMSO in the presence of $Zr(acac)_4$. In some cases, the O-antigen attached to the MSNs was acetylated with acetic anhydride in dry pyridine in the presence of catalytic amounts of DMAP. Cargo was loaded into the MSNs by soaking the samples in an aqueous solution of

the cargo on a shaker overnight. Antibody capping was done by incubating the samples in the presence of FB11 anti-O-antigen antibody and BSA in PBS buffer.

The *wzy* gene, which codes for O-antigen polymerase, was deleted from *F. tularensis* LVS by the method of allelic exchange as described.[33]

LPS and purification of the O-antigen tetrasaccharide was done employing a modification of the methods of Vinogradov *et al.*[34]

Detailed experimental procedures and further details on the employed materials and characterization methods can be found in the supporting information.

3. Results and Discussion

It has been shown that the FB11 antibody recognizes a specific tetrasaccharide sequence at the end of the O-Antigen polysaccharide chain of the Ft-LPS.[35] In our first attempts at pathogen-specific cargo release, we followed a protocol from Vinogradov *et al.* to hydrolytically cleave purified LPS from *Francisella tularensis* live vaccine strain (Ft-LVS-LPS) and extracted the immunoreactive tetrasaccharide units.[34] However, the hydrolysis of the LPS always led to a decrease in immunogenicity, and triggered release of a model drug was not observed after attaching the tetrasaccharides to the nanoparticles by coupling one of the free OH groups to glycidoxypropyl- or isocyanatopropyl groups on the silica surface, capping with FB11 antibody, and adding pristine Ft-LVS-LPS. We also tried longer O-Antigen fragments consisting of 2-3 and ≥5 tetrasaccharide units (obtained from a partial hydrolysis of the LPS), but again, triggered release was not observed.

As we assumed that the loss of immunogenicity of the O-Antigen tetrasaccharide that occurred in the hydrolysis steps (and presumably also in the attachment of the antigen to the nanoparticle surface) interfered with successful antibody capping, we next tried coupling the unmodified, unhydrolyzed Ft-LVS-LPS to the nanoparticles. Two different attachment strategies were developed: one involved binding of the carboxylic acid group of a Kdo sugar (3-Deoxy-D-manno-oct-2-ulosonic acid) in the core region of the Ft-LVS-LPS to aminopropyl-functionalized MSNs through an EDC/NHS amidation reaction; the other strategy again used the attachment of sugar OH-groups to isocyanatopropyl-functionalized MSNs in the presence of a Lewis acid (Zirconium(IV) acetylacetonate) in a dipolar-aprotic, anhydrous solvent (DMSO) (Figure 2.a). To confirm successful attachment of the Ft-LVS-LPS to the surface of the nanoparticles and to assure that the immunogenicity and antibody-binding capability of the Ft-LVS-LPS were retained during the coupling reactions, we used an immunostaining assay to detect the presence of the FB11 antibody that was binding the antigen on the nanoparticle surface (Figure 2.b). Several control experiments were also carried out to make sure that both the antigen and antibody were bound to the MSNs. No immunostaining was observed when either the O-Antigen attachment step, the FB11 binding step, or both were omitted, proving that there is no nonspecific binding of the FB11 antibody to the unfunctionalized MSN surface, and also no non-specific binding of the fluorescent secondary goat-anti-mouse (GAM) immunostaining antibody to the unfunctionalized MSN surface or the Ft-LVS-LPS. From these data, we concluded that both Ft-LVS-LPS antigen attachment and FB11 antibody binding to surface-bound Ft-LVS-LPS were successful.

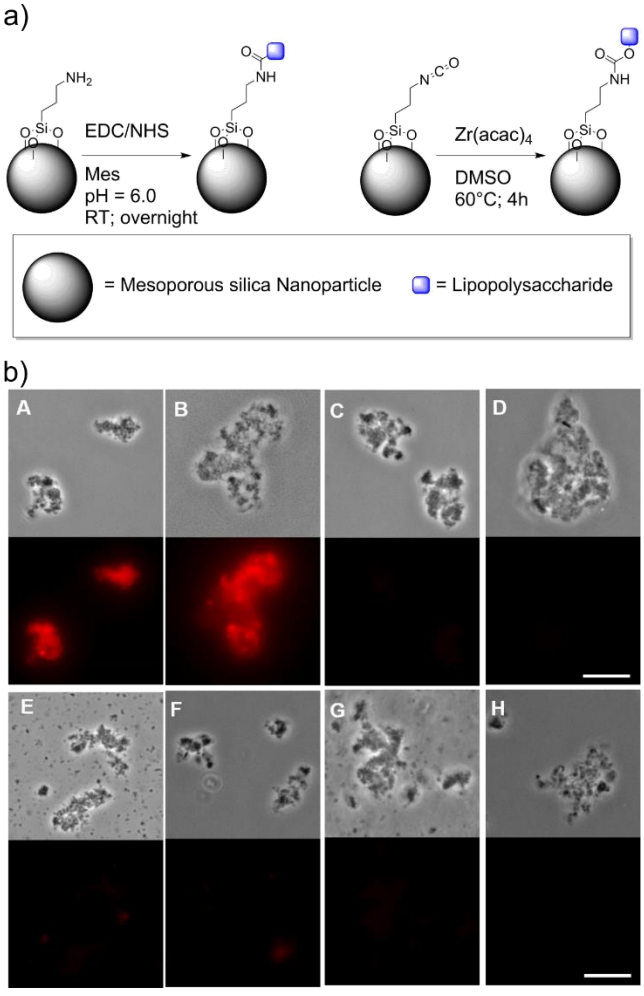

Figure 2. a) Chemical attachment strategies to bind Ft-LVS-LPS to the surface of mesoporous silica nanoparticles. b) Phase contrast (upper part of each panel) and fluorescence (lower part of each panel) microscopy images recorded at fixed exposure and gain settings after Texas Red conjugated GAM immunostaining. (A) Isocyanato-functionalized MSNs with covalently bound LPS that were also incubated with FB11 antibody. (B) Amine-functionalized MSNs with covalently bound LPS that were also incubated with FB11 antibody. (C) Isocyanato-functionalized MSNs with covalently bound LPS, but without FB11 antibody. (D) Amine-functionalized MSNs with covalently bound LPS, but without FB11 antibody. (E) Isocyanato-functionalized MSNs without LPS, incubated with FB11 antibody. (F) Amine-functionalized MSNs without LPS, incubated with FB11 antibody. (G) Isocyanato-functionalized MSNs without LPS and without FB11 antibody. (H) Amine-functionalized MSNs without LPS and without FB11 antibody. The magnification is identical for all images (scale bar: 10μm).

Next, we focused on determining if a competitive displacement of the FB11 antibodies could be triggered in the presence of Ft-LVS-LPS. For this and all future experiments, we decided to use the LPS attachment *via* the Kdo residue to amine-functionalized MSNs through amide bond formation (even though our immunostaining experiments indicated that both attachment strategies worked equally well), since this attachment is experimentally easier and the location of the attachment site is better defined than the random attachment that occurs *via* one of the OH groups to isocyanato-functionalized MSNs. Also, an attachment to a sugar in the core region should not interfere with antibody-antigen binding, while the attachment of the antigen by one of the OH groups of the terminal tetrasaccharide might do so under certain circumstances. We prepared MSNs that were functionalized with Ft-LVS-LPS, capped with FB11 antibodies, and then incubated with either 10^9 live Ft-LVS bacteria or with PBS as a control. Subsequent immunostaining with GAM antibodies did not show a significant reduction in fluorescence of the sample incubated with Ft-LVS bacteria as compared with the control sample. Since the LPS on the MSN surface is identical to the LPS produced by the bacteria, the driving force for a competitive displacement of the antibody appeared to be too low under these conditions. As a proof of principle, we repeated the experiment with a 20 times higher Ft-LVS concentration and for a longer time, and indeed we could see a reduction of fluorescence after GAM immunostaining (Figure S2). These results indicated that the operation of the nanovalve is feasible and that the valve can in principle work at high bacterial (and hence LPS) concentrations *in vitro*.

Next, we focused on strategies to reduce the affinity of the FB11 antibody to the LPS on the MSN surface in order to facilitate the displacement of the antibody at lower Ft bacterial concentrations, which may be more relevant to early stages of an infection. We expected that a covalent modification of the sugars in the O-antigen would lower the binding affinity of the antibody to the O-antigen. More specifically, we anticipated that acetylating the OH groups could lead to a lower binding affinity due to a steric mismatch, a polarity mismatch, and also due to the fact that the acetylated OH groups cannot act as hydrogen bonding donors to the Fab regions of the FB11 antibody any more (they can still act as hydrogen bonding acceptors to some extent). Moreover, the acetylation is experimentally rather simple, inexpensive, and the MSNs can withstand the reaction conditions of the acetylation, as confirmed by transmission electron microscopy (TEM) analysis (Figure S3). This approach also has the advantage that the acetylation can be performed after the coupling of the LPS to the MSNs, making workup easier and keeping open the option of attaching the LPS *via* one of its OH groups, e.g. to isocyanato-functionalized MSNs. Indeed, immunostaining results indicated that FB11 antibodies bound to acetylated LPS on the MSN surface could be displaced after incubation with Ft-LVS-LPS at a concentration of 5 mg/mL (Figure S4). In later experiments, we found that even lower concentrations were sufficient (for example 1.25 mg/mL as demonstrated in Figure 4.b)

Next, we sought to determine if we can use this system to encapsulate cargo molecules and specifically release them in the presence of Ft-LVS-LPS. We prepared a sample in which we attached Ft-LVS-LPS to amine-functionalized MSNs through an amide bond, acetylated the bound LPS, loaded the particles with fluorescein as a model drug and fluorescent indicator, capped the pores with FB11 antibodies, incubated them with Ft-LVS-LPS to trigger the competitive displacement, and measured the amount of released fluorescein. However, despite the fact that earlier immunostaining experiments had shown that LPS attachment and FB11 binding both occur and that a competitive displacement of FB11 from acetylated LPS on the MSN surface can be achieved, the difference between fluorophore release from the sample that was incubated with Ft-LVS-LPS and the control sample was not very pronounced. After several optimization steps, we achieved an approximately 35% greater amount of fluorescein release after 3 h of incubation with Ft-LVS-LPS (2.5mg/mL) compared with a control sample in which no Ft-LVS-LPS was present (Figure S5).

Our next goal was to achieve a better release performance, *i.e.* a larger difference between the amount of cargo released in the presence and absence of Ft-LVS-LPS. In the previous release experiments, we had seen that there was also fluorescein release from the control sample. We assumed that this "leakiness" was due to the fact that the antibody was too far away from the nanoparticle surface and the pore openings to provide effective capping and hence a sufficient enough barrier to diffusion of guest molecules from the pores of the MSNs into the solution. In the naturally occurring Ft-LVS-LPS the O-antigen unit typically consists of many tetrasaccharide repeating units, which gives rise to a large distance between the core region (where the Kdo sugar and hence the attachment site to the nanoparticles is located) and terminal tetrasaccharide at the end of the O-Antigen chain (where the binding site for the FB11 antibody is located). To bring both sites

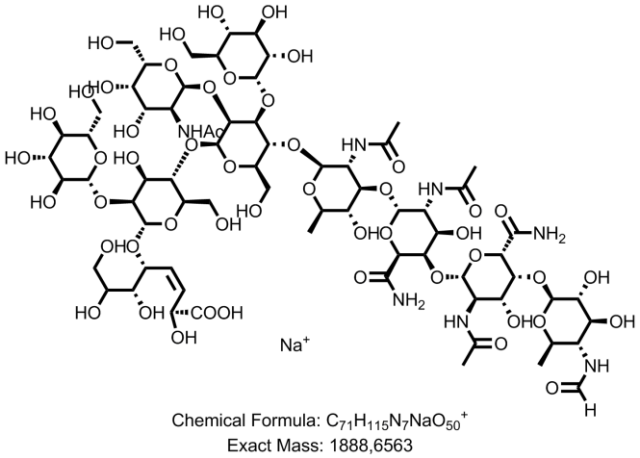

Figure 3. Suggested structure of the sample isolated after careful hydrolysis of the lipid A part of the LPS from a *wzy* deletion mutant of Ft-LVS.

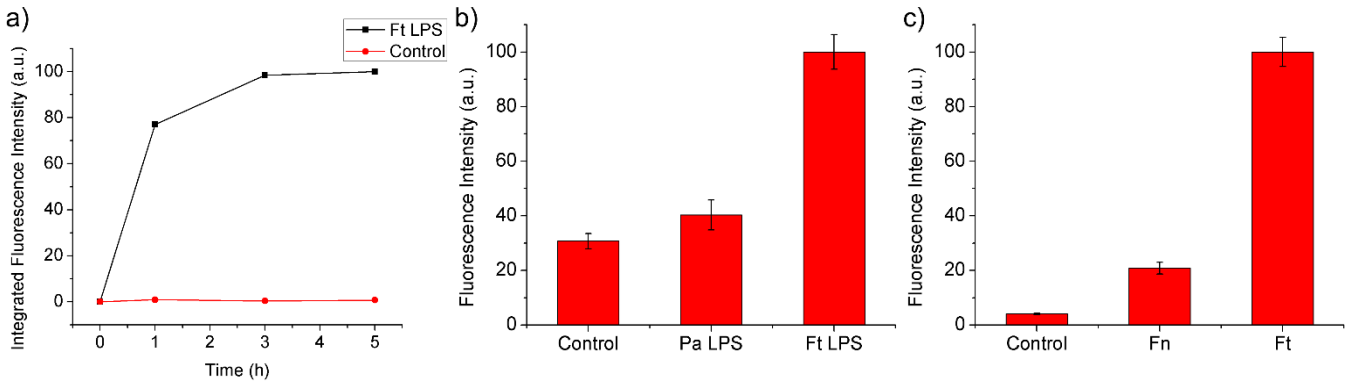

Figure 4. a) Time-based release of a model drug (Hoechst 33342) in the presence (black squares) and absence (red dots) of purified Ft-LVS-LPS (1.25 mg/mL). b) Nuclear staining intensity after release of a model drug (Hoechst 33342) triggered by incubation of MSNs with 1.0 mg/mL purified LPS from *Pseudomonas aeruginosa* (Pa LPS), 1.0 mg/mL *Francisella tularensis* (Ft LPS), and a control sample containing only PBS buffer for 1 h at 37 °C. c) Fluorescence intensity after release of a model drug (Hoechst 33342) in vitro triggered by incubation of MSNs with live *Francisella novocida* bacteria (Fn), live *Francisella tularensis* bacteria (Ft), and a control sample containing only PBS for 1 h at 37 °C.

closer together, we decided to use LPS from a Ft *wzy* deletion mutant (Figure S6). This mutant lacks a gene that encodes an enzyme that polymerizes the O-antigen chain, *i.e.* the LPS of these mutants consists of the lipid A part, the core region, and only one tetrameric unit of the O-antigen. We obtained the single tetrasaccharide-containing LPS after introducing the *wzy* mutation into *F. tularensis* LVS, growing the bacteria, extracting and purifying their LPS, and carefully hydrolyzing off the lipid A part. The product was characterized by matrix assisted laser desorption ionization time of flight mass spectrometry (MALDI-TOF MS), and a structure consistent with that previously described in the literature for Ft-LVS-LPS was obtained (Figure 3 and Figure S7).[36] The suggested structure ($[M]+Na^+$, m/z_{calcd}=1888.6563, m/z_{found}=1888.6198) differs from the published structure by the fact that a galactosamine in the core region is acetylated and that the Kdo sugar underwent beta-elimination and was reduced, which can be explained by the acidic hydrolysis and the reductive workup, respectively. The peaks at m/z=1910.6321 and m/z=1726.6368 correspond to the exchange of H^+ for Na^+ ($\Delta m/z_{calcd}$=21.9820) and the loss of a hexose sugar ($\Delta m/z_{calcd}$=162.0528) from the suggested structure, respectively. The m/z values and isotope pattern of the main peak are in excellent agreement with the structure suggested in Figure 3.

After confirming the structure and purity of the sample, we used our previously developed and optimized approach to bind the LPS from the *wzy* deletion mutant to amine-functionalized MSNs, acetylated the bound LPS, loaded the MSNs with fluorescein as a model drug, capped the pores with FB11 antibody, and performed another release experiment in which we added natural LPS from the parental non-mutated Ft-LVS bacteria (Figure 4.a). We observed a strong increase in fluorescein release after Ft-LVS-LPS addition indicating that a) leakiness was markedly reduced by use of the shorter LPS produced by the *wzy* deletion mutant; b) cargo was efficiently retained inside the porous MSNs by means of the antibody nanovalve; and c) the MSNs released their cargo upon a specific stimulus, i.e. Ft-LPS. We also checked the selectivity of the nanovalve by comparing the release of a model drug in the presence of Ft-LVS-LPS vs. a different LPS from *Pseudomonas aeruginosa* (Pa) in which the O-Antigen chain (as with Ft) also contains modified galactosamines and quinovosamines. As expected from the highly specific nature of the antibody-antigen interaction, a significant increase in cargo release was observed only in the presence of Ft-LVS-LPS, and not in the presence of Pa-LPS (see Figure 4.b). After these successful preliminary results with the cargo delivery platform, we further tested the specificity of cargo release using the live bacteria by comparing release by Ft with that of the very closely related bacterium *Francisella novocida* (Fn; for a comparison of the very similar O-Antigen structures, see Figure S8). Indeed, a highly selective release of the model drug was observed as MSNs incubated with Ft but not with Fn or medium showed pronounced release (see Figure 4.c). These results demonstrate the feasibility and the high selectivity of this drug delivery platform in vitro.

The FB11 antibody is well suited for capping of the MSN pores because it recognizes the terminal tetrasaccharide of the LPS O-antigen, i.e., the antigen which is most peripheral and therefore most surface exposed, and its displacement is not complicated by steric hindrance. On the other hand, steric hindrance would likely be a factor limiting the use of antibodies that recognize internal O-antigen sugars. Because the FB11 antibody recognizes the terminal sugars, both bacteria-bound LPS and free LPS should be able to displace the antibody from the surface of the MSN. Gram-negative bacteria are well known to shed LPS during normal growth,[37,38] and we have found that this phenomenon holds true for *F. tularensis*, with shedding of 0.2% and 0.6% of their LPS growing on agar plates or broth culture, respectively (supplemental Figure 1). We have also observed abundant shedding of LPS by *F. tularensis* following phagocytosis by macrophages and the

presence of LPS in vesicular compartments separate from *F. tularensis* bacilli.

Direct interaction between the MSNs and the bacteria is not required for the MSNs to kill the bacteria. Indeed, in our previous studies of MSN that release antibiotics after uptake by macrophages, we have demonstrated that the MSN-delivered antibiotics kill intracellular bacteria despite the MSN and the bacteria being located in different intracellular compartments of the macrophage.[39–41] Antibiotics released from the MSNs are able to diffuse into the adjacent medium or the host cell cytosol and kill the bacteria even without direct contact between the MSNs and the bacteria.

4. Conclusion

As discussed in this paper, it is a challenge to design and make a nanomaterial that can selectively and autonomously respond to a specific molecule or organism and signal its presence. In the area of human safety, such a nanomaterial may be useful for detection of toxic substances including poisons, environmental pollutants, man-made chemical warfare agents, and pathogens. The latter, the subject of this paper, can include disease-causing bacteria in general and Ft as a specific bio-warfare or bioterrorism threat.

We presented design considerations and a synthetic approach that allow for highly selective, pathogen-specific triggered cargo release from MSNs with possible applications for the detection and treatment of a target pathogen. We found that the use of LPS from a *wzy* deletion mutant significantly reduced leakage, presumably because it brings the antibody cap closer to the pore openings. The competitive displacement of the antibody caps was made more feasible by acetylating the O-Antigen bound to the nanoparticles without interfering with the structural integrity of the MSNs. We presented the use of a fluorescent dye cargo that provided the signaling event. The use of antibiotics as cargo to kill the bacteria is under current investigation in our laboratories. Since the specificity and triggered release is based on the interaction between antibody and the O-Antigen chain of the LPS, we believe that the same principles can also be applied to a variety of other gram-negative bacteria, providing a new platform for pathogen-responsive cargo delivery for the detection and treatment of infectious diseases.

ASSOCIATED CONTENT

Supporting Information. Detailed experimental procedures, additional figures and characterization data. This material is available free of charge via the Internet at http://pubs.acs.org.

AUTHOR INFORMATION

Corresponding Author

*M. A. Horwitz: mhorwitz@mednet.ucla.edu
*J. I. Zink: zink@chem.ucla.edu

Author Contributions

The manuscript was written through contributions of all authors. All authors have given approval to the final version of the manuscript. ‡These authors contributed equally.

Funding Sources

This work was supported by Defense Threat Reduction Agency Grant HDTRA1-13-1-0046.

ACKNOWLEDGMENT

The authors gratefully acknowledge financial support by Defense Threat Reduction Agency Grant HDTRA1-13-1-0046.

ABBREVIATIONS

DMSO, dimethylsulfoxide; EDC, 1-Ethyl-3-(3-dimethylaminopropyl)carbodiimide; DMAP, 4-(Dimethylamino)-pyridin; Fn, Francisella novocida; Ft, Francisella tularensis; ICPTES, 3-isocyanatopropyl triethoxysilane; LPS, lipopolysaccharide; LVS, live vaccine strain; MALDI-TOF MS, matrix-assisted laser desorption ionization-time of flight mass spectrometry; MSNs, mesoporous silica nanoparticles; NHS, N-hydroxysuccinimide; Pa, Pseudomonas aeruginosa; TEM, transmission electron microscopy.

REFERENCES

(1) Saslaw S; Eigelsbach HT; Prior JA; Wilson HE; Carhart S. *Arch. Intern. Med.* **1961**, *107*, 702.
(2) Chocarro, A.; Gonzalez, A.; Garcia, I. *Clin. Infect. Dis.* **2000**, *31*, 623.
(3) Feldman, K. A.; Enscore, R. E.; Lathrop, S. L.; Matyas, B. T.; McGuill, M.; Schriefer, M. E.; Stiles-Enos, D.; Dennis, D. T.; Petersen, L. R.; Hayes, E. B. *N. Engl. J. Med.* **2001**, *345*, 1601.
(4) Harris, S. *Ann. N. Y. Acad. Sci.* **1992**, *666*, 21.
(5) Christopher LW; Cieslak LJ; Pavlin JA; Eitzen EM; Jr. *JAMA* **1997**, *278*, 412.
(6) Alibek, K.; Handelman, S. *Biohazard: The Chilling True Story of the Largest Covert Biological Weapons Program in the World--Told from the Inside by the Man Who Ran It*, Reprint.; Delta: New York, 2000.
(7) Li, Z.; Clemens, D. L.; Lee, B.-Y.; Dillon, B. J.; Horwitz, M. A.; Zink, J. I. *ACS Nano* **2015**, *9*, 10778.
(8) Lee, B.-Y.; Li, Z.; Clemens, D. L.; Dillon, B. J.; Hwang, A. A.; Zink, J. I.; Horwitz, M. A. *Small* **2016**, *12*, 3690.
(9) Rühle, B.; Saint-Cricq, P.; Zink, J. I. *ChemPhysChem* **2016**, *17*, 1769.
(10) Ambrogio, M. W.; Thomas, C. R.; Zhao, Y.-L.; Zink, J. I.; Stoddart, J. F. *Acc. Chem. Res.* **2011**, *44*, 903.
(11) Tarn, D.; Ashley, C. E.; Xue, M.; Carnes, E. C.; Zink, J. I.; Brinker, C. J. *Acc. Chem. Res.* **2013**, *46*, 792.
(12) Argyo, C.; Weiss, V.; Bräuchle, C.; Bein, T. *Chem. Mater.* **2014**, *26*, 435.
(13) Li, Z.; Barnes, J. C.; Bosoy, A.; Stoddart, J. F.; Zink, J. I. *Chem. Soc. Rev.* **2012**, *41*, 2590.
(14) Tao, L.; Zhang, C.; Zhang, J.; Sun, Y.; Li, X.; Yan, K.; Jin, B.; Zhang, Z.; Yang, K. *Microchim. Acta* **2016**, *183*, 2163.
(15) Ma, H.; Wang, Y.; Wu, D.; Zhang, Y.; Gao, J.; Ren, X.; Du, B.; Wei, Q. *Sci. Rep.* **2016**, *6*, 19797.
(16) Eum, J. Y.; Hwang, S. Y.; Ju, Y.; Shim, J. M.; Piao, Y.; Lee, J.; Kim, H.-S.; Kim, J. *Chem. Commun.* **2014**, *50*, 3546.
(17) Erathodiyil, N.; Ying, J. Y. *Acc. Chem. Res.* **2011**, *44*, 925.
(18) Chiu, H.-Y.; Deng, W.; Engelke, H.; Helma, J.; Leonhardt, H.; Bein, T. *Sci. Rep.* **2016**, *6*, 25019.
(19) Knežević, N. Ž.; Durand, J.-O. *Nanoscale* **2015**, *7*, 2199.

(20) Chen, F.; Nayak, T. R.; Goel, S.; Valdovinos, H. F.; Hong, H.; Theuer, C. P.; Barnhart, T. E.; Cai, W. *Mol. Pharm.* **2014**, *11*, 4007.

(21) Milgroom, A.; Intrator, M.; Madhavan, K.; Mazzaro, L.; Shandas, R.; Liu, B.; Park, D. *Colloids Surf. B Biointerfaces* **2014**, *116*, 652.

(22) Lei, C.; Liu, P.; Chen, B.; Mao, Y.; Engelmann, H.; Shin, Y.; Jaffar, J.; Hellstrom, I.; Liu, J.; Hellstrom, K. E. *J. Am. Chem. Soc.* **2010**, *132*, 6906.

(23) Gao, Y.; Gu, S.; Zhang, Y.; Xie, X.; Yu, T.; Lu, Y.; Zhu, Y.; Chen, W.; Zhang, H.; Dong, H.; Sinko, P. J.; Jia, L. *Small* **2016**, *12*, 2595.

(24) Zhang, Y.; Guo, J.; Zhang, X.-L.; Li, D.-P.; Zhang, T.-T.; Gao, F.-F.; Liu, N.-F.; Sheng, X.-G. *Int. J. Pharm.* **2015**, *496*, 1026.

(25) Zhang, H.; Ding, Q.; Ding, J. *RSC Adv* **2016**, *6*, 5049.

(26) Ngamcherdtrakul, W.; Morry, J.; Gu, S.; Castro, D. J.; Goodyear, S. M.; Sangvanich, T.; Reda, M. M.; Lee, R.; Mihelic, S. A.; Beckman, B. L.; Hu, Z.; Gray, J. W.; Yantasee, W. *Adv. Funct. Mater.* **2015**, *25*, 2646.

(27) Chen, F.; Hong, H.; Shi, S.; Goel, S.; Valdovinos, H. F.; Hernandez, R.; Theuer, C. P.; Barnhart, T. E.; Cai, W. *Sci. Rep.* **2014**, *4*, 5080.

(28) Tsai, C.-P.; Chen, C.-Y.; Hung, Y.; Chang, F.-H.; Mou, C.-Y. *J. Mater. Chem.* **2009**, *19*, 5737.

(29) Climent, E.; Bernardos, A.; Martínez-Máñez, R.; Maquieira, A.; Marcos, M. D.; Pastor-Navarro, N.; Puchades, R.; Sancenón, F.; Soto, J.; Amorós, P. *J. Am. Chem. Soc.* **2009**, *131*, 14075.

(30) Climent, E.; Martínez-Máñez, R.; Maquieira, Á.; Sancenón, F.; Marcos, M. D.; Brun, E. M.; Soto, J.; Amorós, P. *ChemistryOpen* **2012**, *1*, 251.

(31) Climent, E.; Gröninger, D.; Hecht, M.; Walter, M. A.; Martínez-Máñez, R.; Weller, M. G.; Sancenón, F.; Amorós, P.; Rurack, K. *Chem. - Eur. J.* **2013**, *19*, 4117.

(32) Rühle, B.; Datz, S.; Argyo, C.; Bein, T.; Zink, J. I. *Chem. Commun.* **2016**, *52*, 1843.

(33) Clemens, D. L.; Lee, B.-Y.; Horwitz, M. A. *Infect. Immun.* **2012**, *80*, 952.

(34) Vinogradov, E. V.; Shashkov, A. S.; Knirel, Y. A.; Kochetkov, N. K.; Tochtamysheva, N. V.; Averin, S. F.; Goncharova, O. V.; Khlebnikov, V. S. *Carbohydr. Res.* **1991**, *214*, 289.

(35) Roche, M. I.; Lu, Z.; Hui, J. H.; Sharon, J. *Hybrid. 2005* **2011**, *30*, 19.

(36) Gunn, J. S.; Ernst, R. K. *Ann. N. Y. Acad. Sci.* **2007**, *1105*, 202.

(37) Cadieux, J. E.; Kuzio, J.; Milazzo, F. H.; Kropinski, A. M. *J. Bacteriol.* **1983**, *155*, 817.

(38) Mattsby-Baltzer, I.; Lindgren, K.; Lindholm, B.; Edebo, L. *Infect. Immun.* **1991**, *59*, 689.

(39) Li, Z.; Clemens, D. L.; Lee, B.-Y.; Dillon, B. J.; Horwitz, M. A.; Zink, J. I. *ACS Nano* **2015**, *9*, 10778.

(40) Hwang, A. A.; Lee, B.-Y.; Clemens, D. L.; Dillon, B. J.; Zink, J. I.; Horwitz, M. A. *Small Weinh. Bergstr. Ger.* **2015**, *11*, 5066.

(41) Clemens, D. L.; Lee, B.-Y.; Xue, M.; Thomas, C. R.; Meng, H.; Ferris, D.; Nel, A. E.; Zink, J. I.; Horwitz, M. A. *Antimicrob. Agents Chemother.* **2012**, *56*, 2535.

For Table of Contents Only:

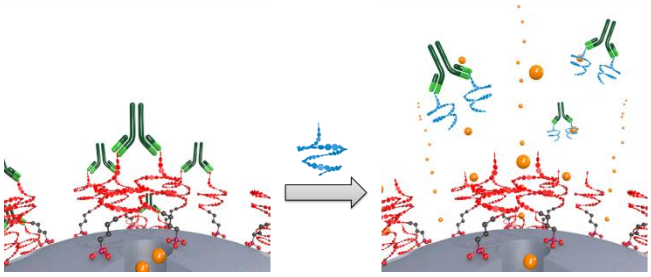

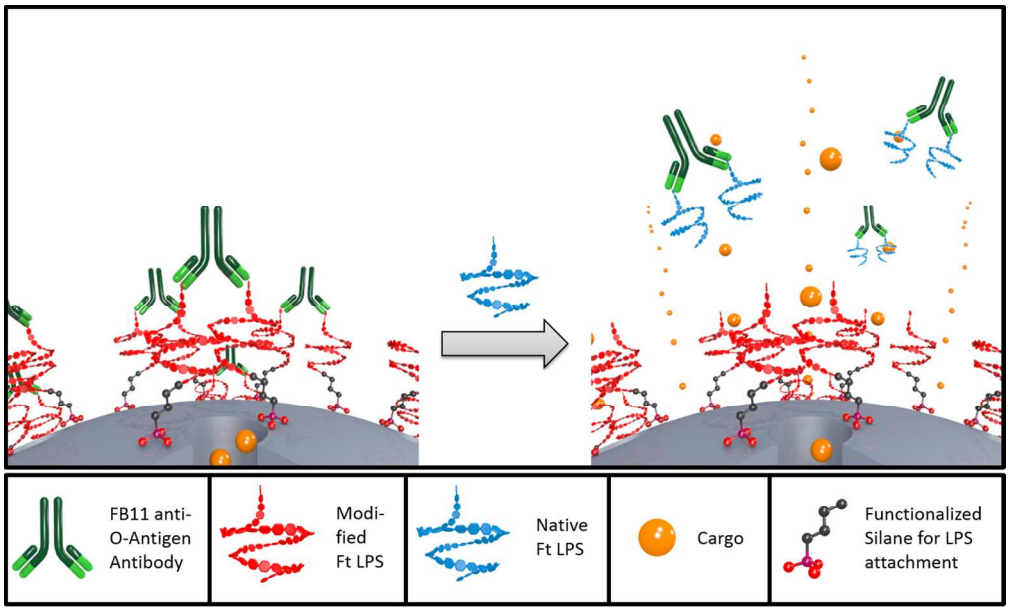

Figure 1. Schematic representation of the triggered release of cargo (orange spheres) loaded into pores due to a competitive displacement of the antibody (green) that caps the pore by naturally occurring Francisella tularensis LPS (blue).

248x149mm (150 x 150 DPI)

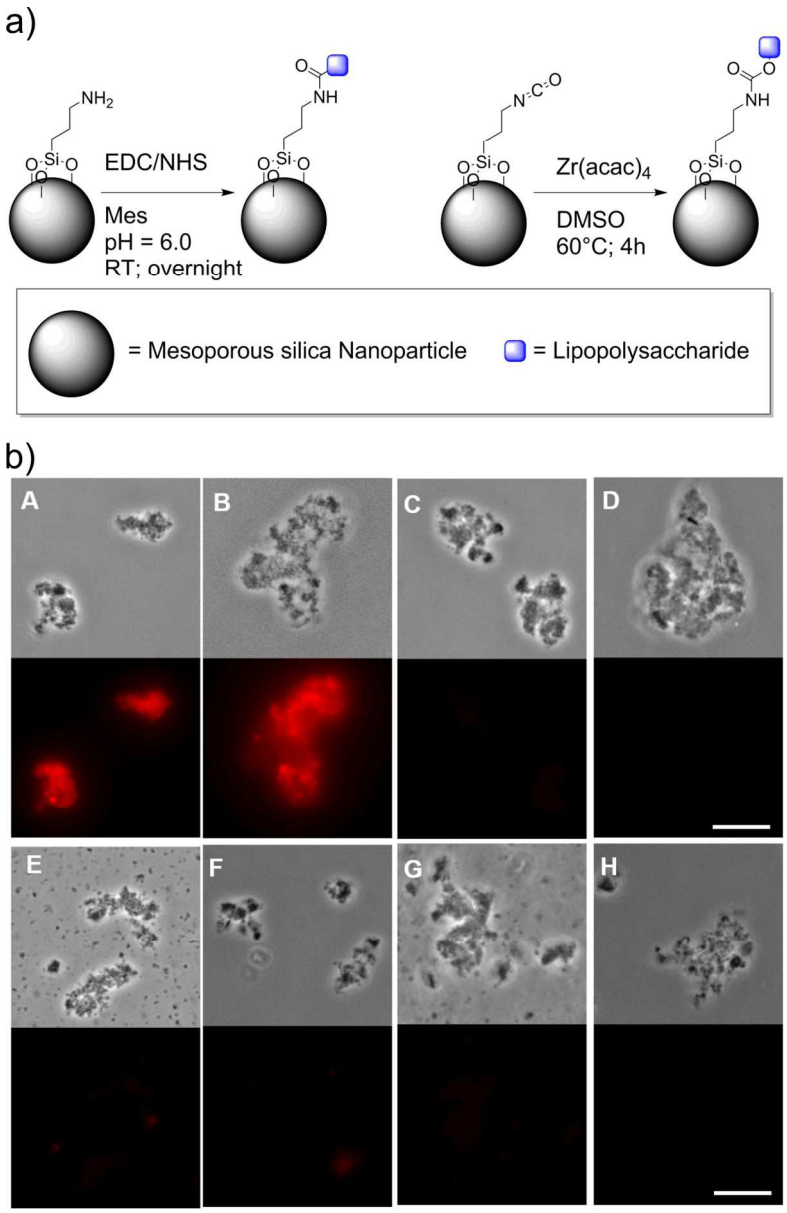

Figure 2. a) Chemical attachment strategies to bind Ft-LVS-LPS to the surface of mesoporous silica nanoparticles. b) Phase contrast (upper part of each panel) and fluorescence (lower part of each panel) microscopy images recorded at fixed exposure and gain settings after Texas Red conjugated GAM immunostaining. (A) Isocyanato-functionalized MSNs with covalently bound LPS that were also incubated with FB11 antibody. (B) Amine-functionalized MSNs with cova-lently bound LPS that were also incubated with FB11 anti-body. (C) Isocyanato-functionalized MSNs with covalently bound LPS, but without FB11 antibody. (D) Amine-functionalized MSNs with covalently bound LPS, but with-out FB11 antibody. (E) Isocyanato-functionalized MSNs without LPS, incubated with FB11 antibody. (F) Amine-functionalized MSNs without LPS, incubated with FB11 anti-body. (G) Isocyanato-functionalized MSNs without LPS and without FB11 antibody. (H) Amine-functionalized MSNs without LPS and without FB11 antibody. The magnification is identical for all images (scale bar: 10µm).

350x541mm (90 x 90 DPI)

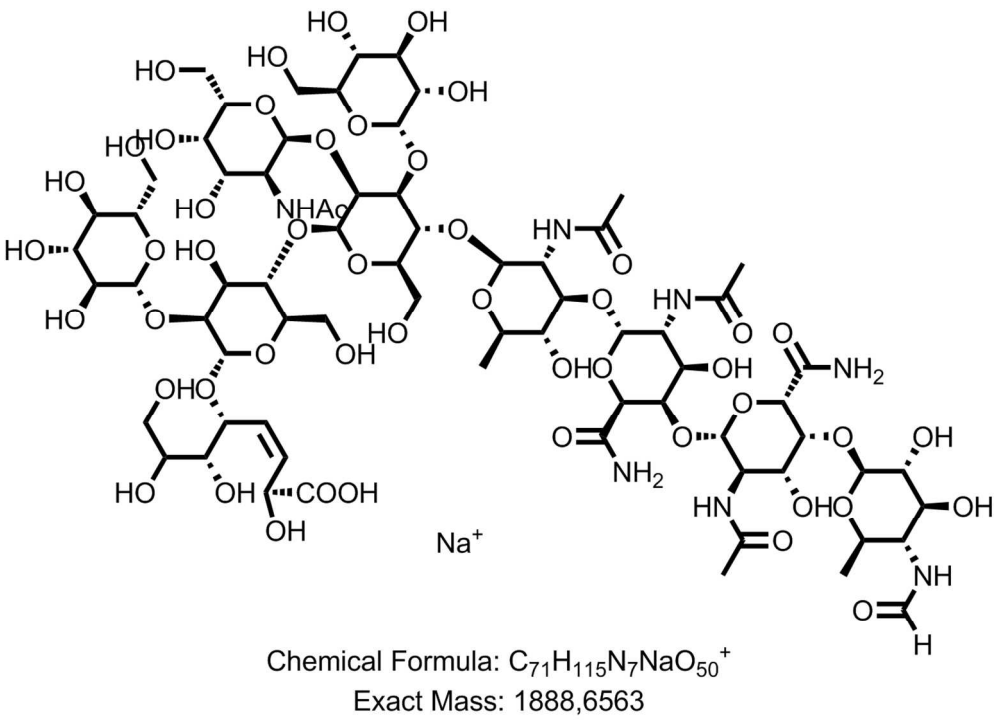

Figure 3. Suggested structure of the sample isolated after careful hydrolysis of the lipid A part of the LPS from a wzy deletion mutant of Ft-LVS.

396x285mm (96 x 96 DPI)

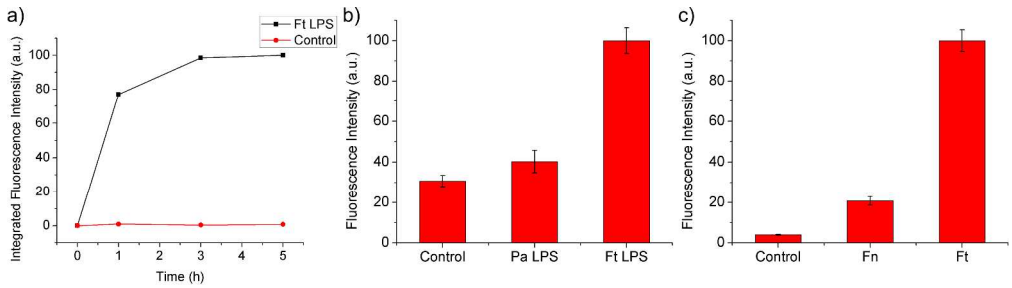

Figure 4. a) Time-based release of a model drug (Hoechst 33342) in the presence (black squares) and absence (red dots) of purified Ft-LVS-LPS (1.25 mg/mL). b) Nuclear staining intensity after release of a model drug (Hoechst 33342) triggered by in-cubation of MSNs with 1.0 mg/mL purified LPS from Pseudomonas aeruginosa (Pa LPS), 1.0 mg/mL Francisella tularensis (Ft LPS), and a control sample containing only PBS buffer for 1 h at 37 °C. c) Fluorescence intensity after release of a model drug (Hoechst 33342) in vitro triggered by incubation of MSNs with live Francisella novocida bacteria (Fn), live Francisella tularensis bacteria (Ft), and a control sample containing only PBS for 1 h at 37 °C.

1599x443mm (90 x 90 DPI)